Nanoscale

www.rsc.org/nanoscale

Volume 5 | Number 3 | 7 February 2013 | Pages 825–1236

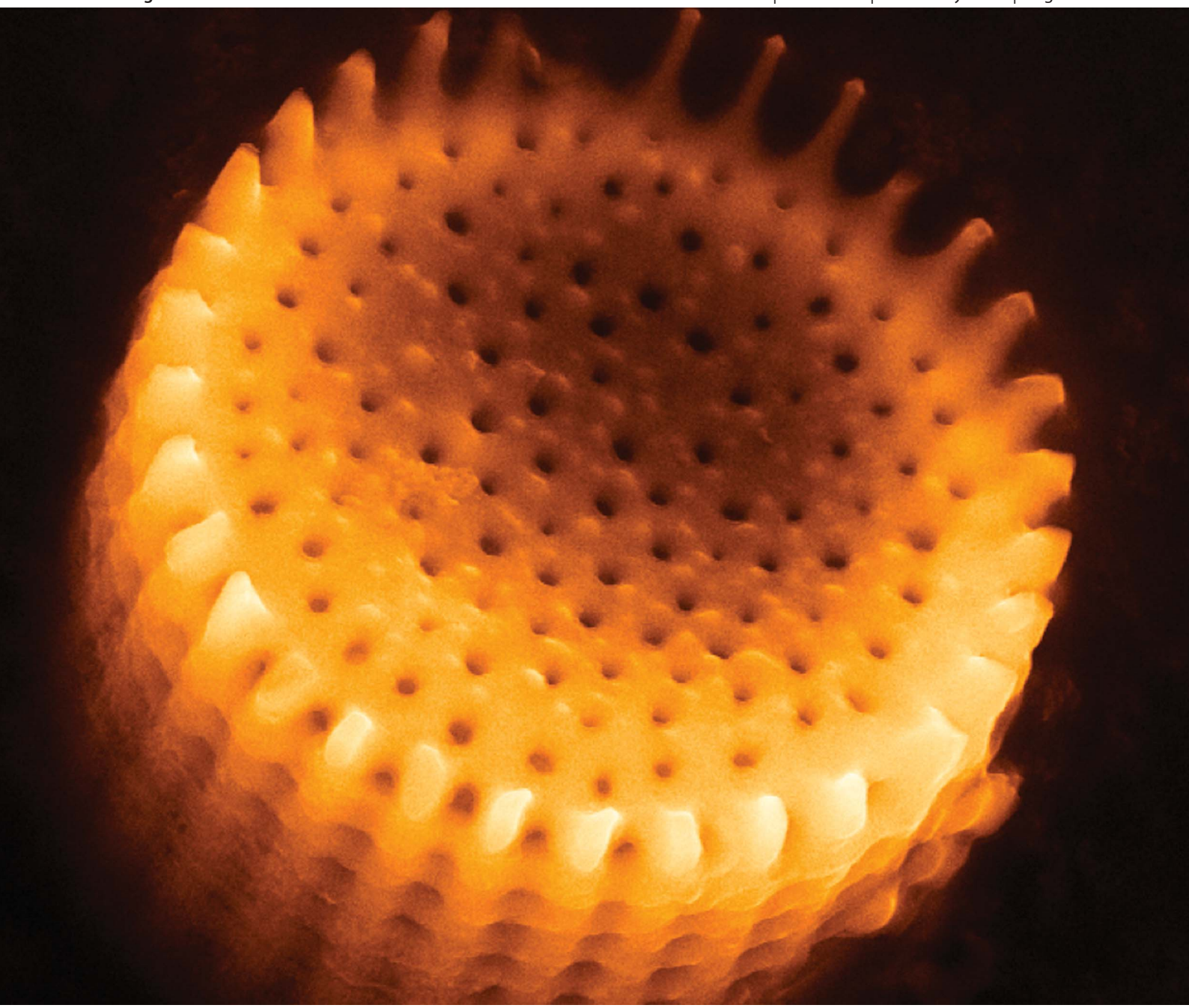

ISSN 2040-3364

RSC Publishing

COMMUNICATION

Raston *et al.*

Diatom frustules as light traps enhance DSSC efficiency

NCNST

Nanoscale

RSC Publishing

COMMUNICATION

Diatom frustules as light traps enhance DSSC efficiency†

Jeremiah Toster,[a] K. Swaminathan Iyer,[a] Wanchun Xiang,[c] Federico Rosei,[b] Leone Spiccia[c] and Colin L. Raston*[a]

Cite this: *Nanoscale*, 2013, **5**, 873

Received 12th September 2012
Accepted 3rd November 2012

DOI: 10.1039/c2nr32716c

www.rsc.org/nanoscale

Diatoms are one of the most successful photosynthetic organisms and given the important role that their shells (frustules) play in light trapping we explored their use in multilayered materials for application as photoanodes in dye sensitised solar cells (DSSCs). We find a substantial improvement in energy conversion efficiency of 30%, increasing from 3.5% to 4.6% with diatom incorporation.

Since their invention in 1991, dye sensitised solar cells (DSSCs) have developed into a promising technology for high solar energy conversion efficiencies at potentially low cost, which can rival the industrially dominant silicon p–n junction photovoltaics.[1–3] DSSCs provide for a less energy intensive and more cost effective manufacturing process than their silicon counterparts, yet are currently held back by lower relative conversion efficiencies.[3] DSSCs use a photosensitive dye (sensitiser), which most commonly is a ruthenium(II) complex, although porphyrins, organic dyes and quantum dots are increasingly used.[1,4–8] The sensitiser is bound to a mesoporous metal oxide semiconductor, typically small transparent titania nanoparticles (~20 nm) which provides a high surface area to allow dense dye attachment. An additional layer of larger metal oxide particles (~400 to 800 nm) is also introduced to help scatter any incoming light passing through the first layer back into the active layer. The semiconductor layers act as a transport medium for the excited electrons generated from the dye.[9,10] On light absorption, electrons are excited into the conduction band of the semiconducting material and then travel to the working electrode, the dye itself being regenerated by an electrolyte, usually containing iodide/tri-iodide as redox mediator.[1,3] Titania is used as the semiconducting material because of its excellent electron conductivity, good matching of the conduction band with the lowest unoccupied molecular orbital (LUMO) of the photosensitive dyes, and tight chemical binding interface.[11] Other metal oxides trialled as possible alternatives include SnO_2, Nb_2O_5 and ZnO.[12–14] There have also been substantial efforts to make use of one dimensional oxide nanostructures such as zinc oxide and titania nanotubes.[9,15] In addition, there have been numerous efforts to dope titania with Zn, Al, Zr and Nb attempting to improve the interaction of the semiconductor with the dye, thereby improving DSSC efficiencies.[16] Hierarchically structured films are effective at improving conversion efficiencies; Zhang *et al.* utilised polydisperse aggregates of nano-sized zinc oxide crystallites with improved DSSC efficiency, from 2.4% to 5.4%, and Memarian *et al.* incorporated a blocking layer resulting in a conversion efficiency of 7.5%, which is currently the leader for zinc oxide DSSC's.[10,17]

Diatoms are photosynthetic microorganisms which are found in marine and fresh water environments.[18,19] They possess species specific hierarchically organised three dimensional porous exoskeletons comprised of silica, which are called frustules. The frustules come in two overlapping halves which separate for reproduction, and generally separate during processing of the frustules for functionalisation. The pores vary in size from 50 nm to in excess of one micron and the organisms themselves can range between a micron to a millimetre depending on the species. The most common species of the mixed diatom sample used for this work was of a cylindrical shape and each half of the organism was approximately 8 μm wide and 12 μm long. Diatoms are responsible for approximately one-fifth of the production of organic compounds from carbon dioxide on Earth and make up a quarter of all plant life by weight.[18,20] The diatom frustule provides an inexpensive avenue for accessing complex 3-dimensional structures designed in nature specifically for scattering and trapping light.[21] Diatoms began evolving in a time when carbon dioxide was scarce in the atmosphere, so they developed the silica frustules which help to concentrate carbon dioxide and allow light into the organism

[a]*Centre for Strategic Nano-fabrication, School of Chemistry and Biochemistry, The University Of Western Australia, Crawley, WA-6009, Australia. E-mail: colin.raston@uwa.edu.au; Fax: +61 8 6488 8683; Tel: +61 8 6488 3045*

[b]*Institut National de la Recherche Scientifique, Université du Quebec, 1650 Boul. Lionel Boulet, J3X1S2, Varennes, QC, Canada. E-mail: rosei@emt.inrs.ca; Fax: +1 450 929 8102; Tel: +1 514 228 8246*

[c]*School of Chemistry and ARC Centre of Excellence for Electromaterials Science, Monash University, Victoria-3800, Australia. E-mail: leonespiccia@monash.edu; Fax: +61 3 9905 4597; Tel: +61 3 9905 4526*

† Electronic supplementary information (ESI) available: Materials and method, AFM of pristine frustules and frustules after a single cycle. XRD of the frustules after 1 cycle and calcination at 500 °C for four hours. See DOI: 10.1039/c2nr32716c

increasing the rate of photosynthesis, making diatoms one of the most successful organisms on the planet. The effectiveness of the light trapping ability of the diatom frustules has been previously reported but the application of titania coated frustules in DSSC remains unexplored.[21]

In this work, we coated the frustules with titania nanoparticles, to improve the light harvesting efficiency of DSSCs, as presented in Fig. 1. Diatom frustules have been previously coated with a thin film of titania and a layer of titania nanoparticles, and have had titania metabolically inserted into their structure at the cultivation stage.[21–23] While these approaches effectively incorporate titania into the frustule pore structure, they are not viable for incorporation into DSSCs. Despite having great connectivity, a thin film of titania lacks the high surface area that nanoparticles provide.[22] Frustules composed entirely of titania would be advantageous but the metabolic insertion is ineffective being only 3.7 wt% of titania relative to silica, and too low to be useful in DSSCs.[21] A nanoparticle coating using a layer-by-layer approach with phytic acid as a molecular binder, achieved remarkable control, but the growth rate is too slow, requiring an inordinate amount of time to perform the number of cycles required to achieve good interparticle contact and to maintain a high short circuit current for DSSCs.[23]

A vital aspect of template directed assembly of nanoparticles is the availability of an effective route to attach nanoparticles to the substrates. Most commonly immobilisation of the nanoparticles is achieved by the modification of the surface with functional groups, such as pyridyl, carboxy, thiol and amino groups, which provide attraction between the nanoparticles and substrate.[24] We present a method for coating the frustules with titania nanoparticles which can be repeated to increase the coverage of the silica substrate and allows for concurrent testing of the light harvesting efficiency after each cycle. By increasing the number of cycles the short circuit current was increased substantially, resulting in significantly improved efficiencies as presented in Table 1.

Once the frustules have been plasma treated no other modification of the surface was required to attach the titania nanoparticles, as shown in Fig. 2. Plasma treatment is a clean and reagentless process in which the frustules were exposed to an air plasma source at a frequency of 40 kHz at 110 W for three five minute periods, with agitation between each ion bombardment. This technique is known to effectively remove methyl groups bound to a silica surface and to help form hydrophilic hydroxyl groups that can bind effectively with titania.[25] The titania was synthesised at room temperature *via* the controlled hydrolysis of titanium(IV) isopropoxide (TIP) in purged hexane. Hydrolysis was carried out by injecting hydrated air into a solution of hexane (100 mL) and TIP (200 μL) containing plasma treated diatom frustules (80 mg). Subsequently the frustules were calcined at 500 °C for four hours, resulting in surface bound anatase nanoparticles ≤20 nm in diameter, as shown by the TEM images, in Fig. 2, and AFM images (ESI†), and calculated by using the Scherrer equation from the X-ray diffraction data (XRD), (ESI†). From the XRD data it was also established that the titania is in the anatase phase, by the primary anatase (101) peak at 25.3° and the absence of the rutile (110) peak at around 27°. The nanoparticles are slightly larger compared to those obtained using other techniques, but are suitable for DSSC's when using an iodide/tri-iodide redox mediator, noting Chou *et al.* established that approximately 23 nm particles have improved efficiencies than approximately 10 nm particles.[26–28] The process was then repeated to increase the thickness and connectivity of the titania coating. Titania coated diatoms, calcined at 500 °C for 4 hours, were made into a paste using ethyl cellulose and terpineol (2 : 1 : 7 diatom/titania : ethyl cellulose : terpineol). The paste was screen printed onto FTO glass and calcined at 500 °C for 2 hours. The working electrode was immersed into a solution of the N719 ruthenium dye overnight and then washed with ethanol, sealed to a platinum counter electrode and back filled with the iodide/tri-iodide electrolyte (cell construction followed general published

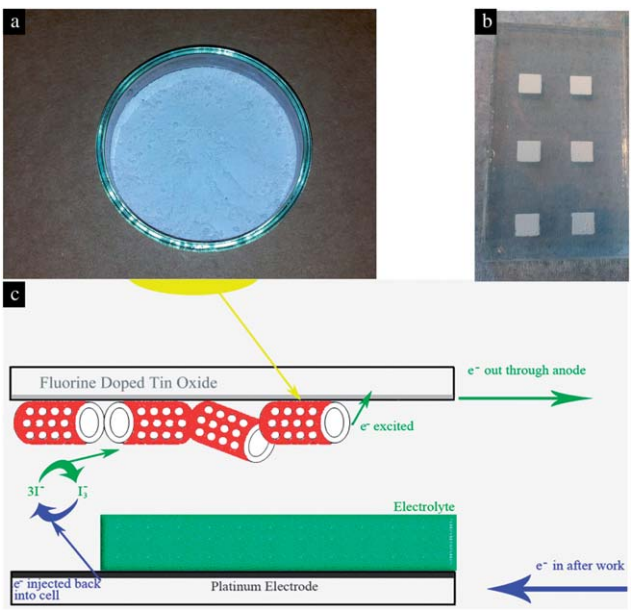

Fig. 1 Image of diatomaceous earth (a) and the working electrode made by screen printing the diatom paste (b). Schematic of the DSSC incorporating diatomaceous earth (c).

Table 1 Efficiencies of DSSC constructed with titania coated diatoms and, for comparison, titania prepared using the same methodology[a]

	V_{oc} (mV)	J_{sc} (mA cm^{-2})	FF (%)	η (%)
Diatom	792	0.14	56.0	0.06
1 Cycle	817 ± 5	4.1 ± 0.3	75.1 ± 1.5	2.5 ± 0.1
2 Cycles	816 ± 3	7.1 ± 0.4	73.3 ± 0.3	4.3 ± 0.3
3 Cycles	804 ± 5	7.7 ± 0.3	74.0 ± 0.5	4.6 ± 0.2
4 Cycles	814 ± 21	7.6 ± 0.4	72.0 ± 0.3	4.5 ± 0.1
Titania only[b]	808 ± 13	5.9 ± 0.5	73.0 ± 0.2	3.5 ± 0.3

[a] Electrolyte containing 0.6 M 1-butyl-3-methylimidazolium iodine (BMII), 0.03 M I_2, 0.5 M 4-*tert*-butylpyridine and 0.1 M guanidinium thiocyanate in acetonitrile and valeronitrile (85 : 15 vol%) solvent mixture. Ruthenium dye N719 (0.3 mM in acetonitrile and *tert*-butanol (50 : 50 vol%)) was used as sensitizer. The film thicknesses for titania only, 3 cycle and 2 cycle were all approximately 26 μm while 1 cycle and diatom only films averaged closer to 37 μm. [b] Prepared *via* the controlled hydrolysis of titanium(IV) isopropoxide in purged hexane. Cell performance as reported is the average of at least three devices.

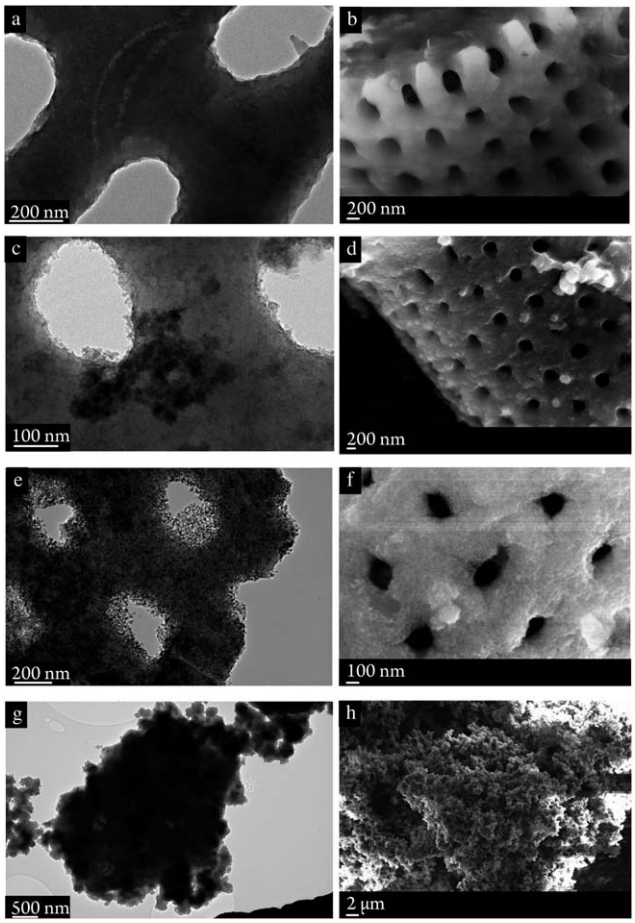

Fig. 2 TEM (left) and SEM (right) of pristine diatoms (a and b) and titania coated diatoms after 1 cycle (c and d), 2 cycles (e and f) and 3 cycles (g and h).

procedures).[29] By increasing the number of titania deposition cycles, the short circuit current significantly improved as detailed in Table 1, where the open circuit voltage (V_{oc}), short circuit current density (J_{sc}), fill factor (FF) and efficiencies (η) are reported (Fig. 3).

Use of photoanodes consisting of dye absorbed on diatom frustules in the absence of titania resulted in low performance devices, which have low short circuit current densities and efficiencies, as expected given the insulating properties of silica. After one cycle of titania nanoparticle deposition, there is a dramatic improvement in the efficiency. The TEM images in Fig. 2c and d show titania on the surface but the frustule coverage and interconnection between titania particles is incomplete. The second cycle provided another substantial leap in efficiency of over 70%. Here, the higher density of particles on the surface with greater interparticle contact is evident from the SEM image in Fig. 2(f). After the third cycle, the diatom frustules become difficult to distinguish using SEM and TEM as they get engulfed by titania, as evident in Fig. 2g and h, and there is clearly a greater interconnectivity between different frustules. This is reflected in an increase in the DSSC efficiency to 4.6%, a slight improvement on the two cycle system. The greater interconnectivity may be countered by a loss in some ordered structure the diatoms provide resulting in the small increase. A fourth cycle of titania coating showed no noticeable improvement (4.5%) upon the third cycle (4.6%) likely due to maximum connectivity already being reached and further cycles are likely to completely negate the structure of the diatom by the overwhelming amount of titania. For comparison, an average efficiency of 3.5% was measured for devices assembled with titania particles, prepared by the same method, in the absence of the frustules (Table 1), *i.e.*, in hexane with TIP hydrolysis. The 30% improvement for the cell incorporating the diatom frustules can be attributed to enhanced light scattering and trapping. When light strikes a diatoms frustule, the pores cause multiple reflections thereby increasing the probability for photons to be absorbed by the dye and increasing injection into the semiconductor. Improvement over titania only cells occurred after the second cycle of coating, noting that there is a small improvement in the short circuit current density for the third cycle after which a plateau appears to have been reached. This is consistent with a progressive improvement in contact between titania nanoparticles assembled on the frustule surface and with the FTO substrate, which potentially results in the formation of continuous electron pathways that leads to a reduction in recombination of the electron injected into the semiconductor and either the dye or tri-iodide present in the electrolyte. This is supported by measurements of the Incident Photon-to-Electron Conversion Efficiency (IPCE, see ESI†) which show that the titania–diatoms obtained by treatment with TIP two or more times result in devices with higher conversion efficiencies than the devices made with standard titania only and diatoms subjected to one cycle of TIP treatment.

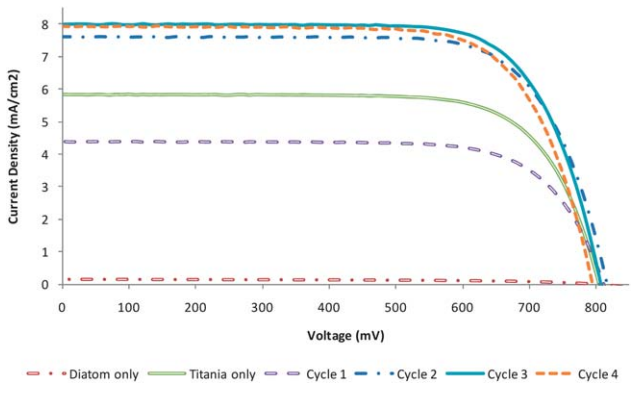

Fig. 3 *I–V* curves for diatom only, titania only and titania coated diatoms, cycles 1–4.

In conclusion, we have established a facile method of effectively coating diatom frustules with titania nanoparticles of less than 20 nm, fundamentally creating three-dimensional titania structures. The *in situ* synthesis of the titania nanoparticles bound effectively to the plasma treated frustules is without the requirement of any linking agents. We observed a significant improvement in conversion efficiency as more cycles were completed resulting in a 30% increase in efficiency compared to the standard titania cell. The synthesis procedure was carried out at room temperature, in hexane, making it far simpler and more economical than many other methods used today.[27,28] The improvement in efficiency, the simplicity of coating and the inexpensive availability make diatoms a viable addition to current DSSC technology.

Acknowledgements

The authors graciously acknowledge the support of the Australian Research Council (ARC) for their funding support of this research, and Mt Silvia Diatomite for the supply of diatoms. The SEM and TEM work was carried out at the Centre for Microscopy, Characterisation and Analysis, UWA. F.R. acknowledges partial salary support from the Canada Research Chairs program. F.R. is grateful to the Institute of Advanced Studies of UWA for a Professor at Large award (2010–2012).

Notes and references

1 B. Oregan and M. Gratzel, *Nature*, 1991, **353**, 737–740.
2 M. Gratzel, *J. Photochem. Photobiol., A*, 2004, **164**, 3–14.
3 M. Grätzel, *J. Photochem. Photobiol., C*, 2003, **4**, 145–153.
4 W. M. Campbell, A. K. Burrell, D. L. Officer and K. W. Jolley, *Coord. Chem. Rev.*, 2004, **248**, 1363–1379.
5 W. M. Campbell, K. W. Jolley, P. Wagner, K. Wagner, P. J. Walsh, K. C. Gordon, L. Schmidt-Mende, M. K. Nazeeruddin, Q. Wang, M. Grätzel and D. L. Officer, *J. Phys. Chem. C*, 2007, **111**, 11760–11762.
6 K. Hara, T. Sato, R. Katoh, A. Furube, T. Yoshihara, M. Murai, M. Kurashige, S. Ito, A. Shinpo, S. Suga and H. Arakawa, *Adv. Funct. Mater.*, 2005, **15**, 246–252.
7 M. Velusamy, K. R. Justin Thomas, J. T. Lin, Y.-C. Hsu and K.-C. Ho, *Org. Lett.*, 2005, **7**, 1899–1902.
8 P. Yu, K. Zhu, A. G. Norman, S. Ferrere, A. J. Frank and A. J. Nozik, *J. Phys. Chem. B*, 2006, **110**, 25451–25454.
9 O. K. Varghese, M. Paulose and C. A. Grimes, *Nat. Nanotechnol.*, 2009, **4**, 592–597.
10 Q. Zhang, T. R. Chou, B. Russo, S. A. Jenekhe and G. Cao, *Angew. Chem., Int. Ed.*, 2008, **47**, 2402–2406.
11 X. Lue, X. Mou, J. Wu, D. Zhang, L. Zhang, F. Huang, F. Xu and S. Huang, *Adv. Funct. Mater.*, 2010, **20**, 509–515.
12 K. K. Wong, A. Ng, X. Y. Chen, Y. H. Ng, Y. H. Leung, K. H. Ho, A. B. Djurisic, A. M. C. Ng, W. K. Chan, L. Yu and D. L. Phillips, *ACS Appl. Mater. Interfaces*, 2012, **4**, 1254–1261.
13 H. J. Snaith and C. Ducati, *Nano Lett.*, 2010, **10**, 1259–1265.
14 P. Guo and M. A. Aegerter, *Thin Solid Films*, 1999, **351**, 290–294.
15 A. B. F. Martinson, J. W. Elam, J. T. Hupp and M. J. Pellin, *Nano Lett.*, 2007, **7**, 2183–2187.
16 X. Lü, X. Mou, J. Wu, D. Zhang, L. Zhang, F. Huang, F. Xu and S. Huang, *Adv. Funct. Mater.*, 2010, **20**, 509–515.
17 N. Memarian, I. Concina, A. Braga, S. M. Rozati, A. Vomiero and G. Sberveglieri, *Angew. Chem., Int. Ed.*, 2011, **50**, 12321–12325.
18 C. Bowler, A. E. Allen, J. H. Badger and J. Grimwood, *et al.*, *Nature*, 2008, **456**, 239–244.
19 F. Noll, M. Sumper and N. Hampp, *Nano Lett.*, 2002, **2**, 91–95.
20 M. W. Anderson, S. M. Holmes, N. Hanif and C. S. Cundy, *Angew. Chem., Int. Ed.*, 2000, **39**, 2707–2710.
21 C. Jeffryes, T. Gutu, J. Jiao and G. L. Rorrer, *ACS Nano*, 2008, **2**, 2103–2112.
22 D. Losic, G. Triani, P. J. Evans, A. Atanacio, J. G. Mitchell and N. H. Voelcker, *J. Mater. Chem.*, 2006, **16**, 4029–4034.
23 Y. X. Jia, W. Han, G. X. Xiong and W. S. Yang, *J. Colloid Interface Sci.*, 2008, **323**, 326–331.
24 S. Malynych, I. Luzinov and G. Chumanov, *J. Phys. Chem. B*, 2002, **106**, 1280–1285.
25 S. Bhattacharya, A. Datta, J. M. Berg and S. Gangopadhyay, *J. Microelectromech. Syst.*, 2005, **14**, 590–597.
26 T. P. Chou, Q. Zhang, B. Russo, G. E. Fryxell and G. Cao, *J. Phys. Chem. C*, 2007, **111**, 6296–6302.
27 E. Scolan and C. Sanchez, *Chem. Mater.*, 1998, **10**, 3217–3223.
28 Y. Li, T. J. White and S. H. Lim, *J. Solid State Chem.*, 2004, **177**, 1372–1381.
29 T. Daeneke, T. H. Kwon, A. B. Holmes, N. W. Duffy, U. Bach and L. Spiccia, *Nat. Chem.*, 2011, **3**, 211–215.

